Structural Engineering and Mechanics, Vol. 39, No. 6 (2011) 849-860
DOI: http://dx.doi.org/10.12989/sem.2011.39.6.849

Experimental investigation on the buckling of thin cylindrical shells with two-stepwise variable thickness under external pressure

Sirous Aghajari[1], Hossein Showkati*[2] and Karim Abedi[1]

[1]*Faculty of Civil Engineering, Sahand University of Technology, Tabriz, Iran*
[2]*Department of Civil Engineering, Urmia University, Urmia, Iran*

(Received January 13, 2010, Accepted June 24, 2011)

Abstract. The buckling capacity of the cylindrical shells depends on two geometric ratios of *L/R* and *R/t*. However the effect of thickness variation on the behavior of the shells is more complicated and the buckling strength of them is sensitive to the magnitude and shape of geometric imperfections. In this paper the effects of thickness variation and geometric imperfections on the buckling and postbuckling behavior of cylindrical shells are experimentally investigated. The obtained results are presented under the effect of uniform lateral pressure. It is found in this investigation that the buckling mode can be generated in the whole length of the shell, if the thickness variation is low.

Keywords: cylindrical shells; experiments; buckling; post buckling; varying thickness; uniform external pressure

1. Introduction

Thin walled shell constructions are used in different industrial applications. The interest is largely due to their extensive use in tanks and silos, offshore structures, aeronautical and aerospace technology, ship hulls, pipelines and industrial chemical plant (Wintersetter and Schmit 2002, Popov 2003, Gadalla and El Kadi 2009). The variation of shell thickness is fully effective on buckling capacity under the effect of lateral pressure. Based on nonlinear correlations obtained by Donnell (1933), the critical capacity of cylindrical shells are dependent on geometric slender ratio of length to radius (*L/R*) and radius to thickness (*R/t*).

There is vast literature devoted to the analysis of geometrically imperfect cylindrical shells. Koiter's general postbuckling theory (Koiter 1967, 1976) provides a basis for analysis of geometric imperfection sensitivity, using the higher order quadratic terms of potential energy on the postbuckling behavior of a structure. It is shown by Hui (1988) that the inclusion of all these higher order terms is essential for an accurate postbuckling analysis. All of imperfection analyses were done on the shells of constant thickness. Lee (1962) studied inelastic buckling of initially imperfect cylindrical shells subjected to axial compression. Hansen (1975) investigated the Influence of

*Corresponding author, Ph.D., E-mail: h.showkati@urmia.ac.ir

general imperfections in axially loaded cylindrical shells. Ansourian (1992) presented simplified design method about imperfections and boundary constraints effects subjected to wind loading. The effect of wind loading is investigated by Portela and Godoy (2007) as well. Holst *et al*. (1999) investigated the method of considering the strains resulted by fabrication misfit of perfect and imperfect shells to attain equivalent residual stresses. Shen and Chen (1991) studied buckling and postbuckling behavior of perfect and imperfect shells with finite length which were subjected to combined axial and external pressure. They showed that this behavior is dependant on geometry, loading and initial imperfections. Then Koiter *et al.* (1994) investigated the influence of modal thickness variation on the buckling load of an axially compressed shell. The thickness variation is assumed to be axisymmetrical and sufficiently small compared to shell thickness. Also Yamaki (1984) have studied the nonlinear behavior of externally pressurized cylindrical shells and effects of geometrical imperfections. Li *et al*. (1997) studied the effects of thickness variation and initial imperfection on buckling of composite cylindrical shells. Gusic *et al*. (2000) have studied the influence of harmonic thickness variation in the circumferential direction on the buckling behavior of thin cylindrical shells under external pressure.

Performing test on manufactured specimens is the most reliable method in engineering research. In this paper, four circular cylindrical shell specimens with a change in thickness have been manufactured and tested. The material was consisted of mild steel with yield stress of 277 MPa. Boundary conditions are all simply supported in which only a radial constrain is provided at the edges. A loading of uniform external pressure is produced by gauged vacuum using suction process. The stages of prebuckling, initial buckling, overall buckling, post buckling and failure of specimens have been observed and evaluated.

2. Experimental program

2.1 Test specimens

For the purpose of this paper, four cylindrical specimens with varying thickness, labeled A, B, C and D, are manufactured and tested under external uniform pressure. The geometry of all models is outlined in Tables 1 and 2. The thickness of specimens is changed in the mid height. The upper half part of specimens A and D has 0.6 mm thickness, while for specimens B and C it is 0.4 mm. Lower parts of all specimens have the same size of 0.8 mm. The total height of specimens A and B is 300 mm and of specimens C and D is 150 mm. All specimens have the same diameter of 600 mm. Two thick steel plates are used at both ends of specimens in which radial groove has been generated to support shell edges. Therefore a simple boundary condition is provided for cylinders

Table 1 Dimensions of test cylinders

Cylinders label	Upper part thickness (mm)	Lower part thickness (mm)	Total height (mm)
A	0.6	0.8	300
B	0.4	0.8	300
C	0.4	0.8	150
D	0.6	0.8	150

Table 2 Slenderness ratios

Cylinders label	$L/2R$	R/t_1	R/t_2
A	0.25	375	500
B	0.25	375	750
C	0.5	375	500
D	0.5	375	750

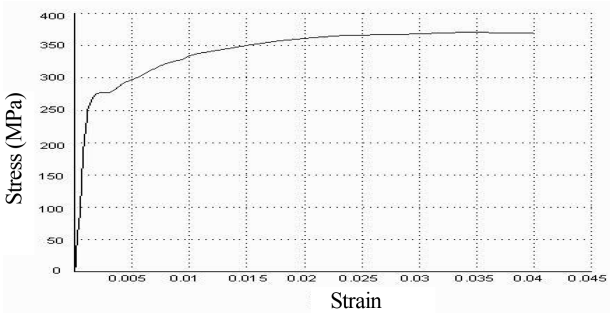

Fig. 1 Stress-strain curve of the material

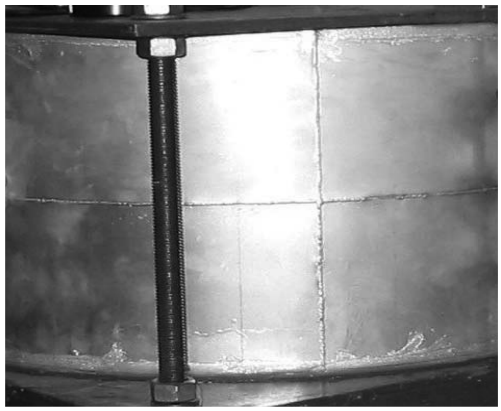

Fig. 2 Vertical and circumferential welding lines

with radial restraint only. Silicon paste was applied around the edges to stop air leakage during vacuum loading.

Three tensile coupon tests were performed to obtain the properties of material of specimens. Fig. 1 shows the resulted stress-strain curve. The yield and failure stresses are 277 and 373 MPa respectively. The Young Modulus is obtained 210 GPa. The Poisson's ratio is assumed to be 0.3.

Each specimen consists of previously rolled sheets which are welded in both vertical and circumferential directions at the edges (Fig. 2). Cooper Fixtures are employed to hold the segments in true place, when the welding is in progress. The thickness variation is located at the center of hoop weld line.

Fig. 3 View of test rig for cylindrical shell and gauges installation and specimens

2.2 Experimental system and instrumentation

The test rig of this study is composed of two parts as shown in Fig. 3. The first part is designed so to hold the test specimen at the desired place by attachment of two horizontal square stiff plates at top and bottom of shell. Circular grooves have been already created on one side of both plates to hold the specimen during the test progress. The upper and lower edges of cylinders were covered by grooved rub and silicon stick was carefully applied over all openings to prevent any possible air leakage during the suction process. Four threaded long bars are provided to adjust the plates for the specimen height as well as to prevent the plates to push the specimen in axial direction. Therefore a simply supported boundary condition was prepared at both ends.

The second part of the rig consisted of a small platform to be used for installation of vacuum pump. This pump is employed to produce uniform external pressure over the shell skin. The loading rate was being controlled using a vent valve which was installed on the top plate. Carefully measured data were collected using several strain gauges, one manometer, two dial gauges and two displacement transducers. Some of the measuring devices are shown in Fig. 3. All the saved data were processed using a data logger system and its special software.

2.3 Preliminary measurements

Cylindrical shells are more sensitive to geometric imperfections in axial load but less sensitive in external pressure. But for the purpose of high accuracy of our results, the initial geometry of specimens was considered in this study by carefully modeling and measurements. It has to be mentioned that the boundary conditions have certain effects on the imperfection analysis of shell structures.

A manual scanning method was used to measure the initial geometry of specimens, in which the circumferential and axial directions are divided to 32 by 480 (32 by 224 for specimens C and D) segments. In each node of obtained mesh, three coordinates of r, θ and z are measured carefully in all specimens. Therefore, a real geometry of shell is obtained and then is used in finite element modeling for further analyses. In Fig. 4 the initial geometry of test shells A, B, C and D are plotted, where x axis shows the circumferential direction.

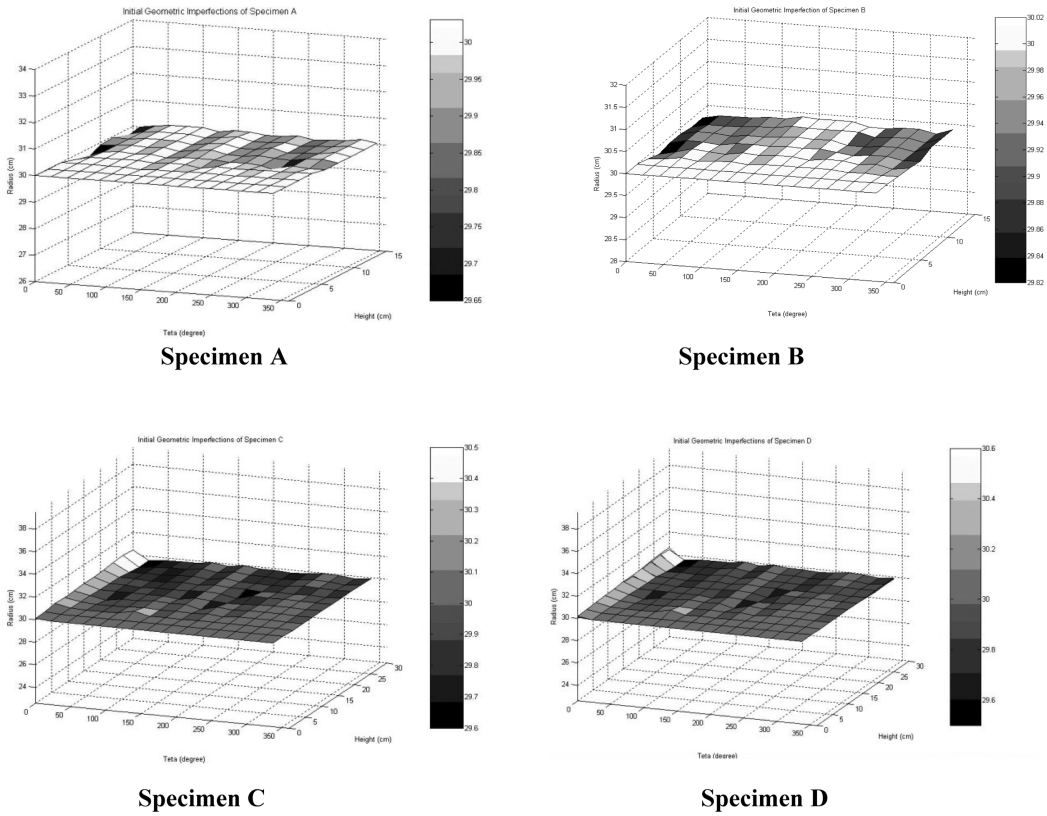

Fig. 4 Initial geometry of test specimens

2.4 Implementation of tests

In this study each of implemented tests was composed of several functions. After installation and calibration of instrumental apparatus, the initial geometric imperfections were measured so to be used in further analysis. Before loading, approximated primary buckling load is calculated by Donnell equation of (1) to determine load steps during the tests. Then, using a vacuum pump, external uniform pressure was applied to specimen until the stage of initial buckling is reached. The next stages of overall buckling and failure mode are then crossed by continuing the suction process. During the test progress, all required data are measured and saved for the further analytical purposes of this paper.

The critical pressure and circumferential buckling mode of all specimens are shown in Table 3 for different test stages. Before initial buckling the behavior of shell was quite elastic with no observed buckle lobe. Donnell equation of (1) calculates the buckling pressure for a cylindrical shell with constant wall thickness, where n is the number of buckling modes. For an approximate case, this Equation is first summarized as Eq. (2) by Batdorf in 1947, later on again by Malik *et al.* (1980) by substituting for $\upsilon = 0.3$. Using Eq. (2), the critical buckling loads (q_{cr}) are calculated for four specimens in two cases of $t_{\min}$ and $t_{\max}$ in each shell, and included in Table 3. Note that $t_{\min}$ and $t_{\max}$ are the thickness of upper and lower half part of each specimen, respectively.

Table 3 Experimental results of buckling tests

Cylinders label	Initial buckling load (kPa)	Overall buckling load (kPa)	Number of buckling modes	Theory (for t_{max})	Theory (for t_{min})
A	31.5	37	9	70.9	34.6
B	11	23	12	70.9	12.5
C	33	40.5	15	141.9	25.1
D	65	74.5	12	141.9	69.1

$$q_{cr} = E\frac{t}{R}\left\{\frac{\left[\left(\frac{\pi R}{L}\right)^2 + n^2\right]^2}{n^2}\cdot\frac{\left(\frac{t}{R}\right)^2}{12(1-\upsilon^2)} + \frac{\left(\frac{\pi R}{L}\right)^4}{n^2\left[\left(\frac{\pi R}{L}\right)^2 + n^2\right]^2}\right\} \tag{1}$$

$$q_{cr} = 0.92E\left(\frac{R}{L}\right)\left(\frac{t}{R}\right)^{2.5} \tag{2}$$

L, R, and t mean the length, radius, and thickness of the cylindrical shell in the Eqs. (1) and (2). At least two rounds of loading and unloading were performed in each test (Aghajari 2005). In first round the external pressure increased slowly up to about 1/3 of buckling load for the purpose of conditioning of the test performance. Then the unloading phase was gradually performed by decreasing vacuum. The main stage of the test implemented at the second round of loading and unloading, in which the buckling and post-buckling states were fully investigated.

The elastic pre-buckling behavior of the shell was carefully assessed before the buckling to be happened. At the stage of post-buckling, the value of external pressure was reached up to full buckling of specimens of A and D and up to failure mode in specimens of B and C. The steps of loading were selected considering the theoretical buckling pressure of Eq. (2) by carefully controlling the pressure increase using vent valve. The two values for an assumed uniform thickness of 0.8 and 0.6 mm are rough estimates for the upper and lower limits of the real theoretical bifurcation pressure of the two-course specimen A. These two calculated buckling pressures using Eq. (2) are 70.9 and 34.6 kPa respectively.

In the test, initial buckling of specimen A with only 3 circumferential full waves occurred at 31.5 kPa. When the pressure reached to 37 kPa a full buckling mode was established with a total of 9 buckling waves. The full buckling pressure almost near to calculated buckling pressures of specimen for thickness of 0.6 mm. The same process was applied for the next specimens of B, C and D to investigate the pre-buckling, initial buckling, overall buckling and post-buckling phases. Each test of this research program was continued until the failure mode of the specimen has happened. The dominated failure mode of specimens was breaking in the boundary conditions which after that the test process is stopped. Table 3 shows the main test results of all specimens in comparison with the theory. In this comparison is concluded the theoretical buckling pressure and mode number are higher than the test results. Because it is not possible to exactly model a physical shell by means of available theory like as Eq. (1). This discrepancy could be increased if the thickness change is present in the shell model.

3. Observations

The behavior of thin shell structures is almost elastic before the initial buckling mode is occurred. In this stage all deformations are disappeared after releasing the pressure. Fig. 5 shows the same behavior for specimens C and D. Thickness variation in tested shells causes the place of maximum radial displacements to be moved into the thinner part of shells. In Fig. 6 a comparison is made between initial and final geometry of test specimen A, in which the maximum deformation is located on the height of 3/4.

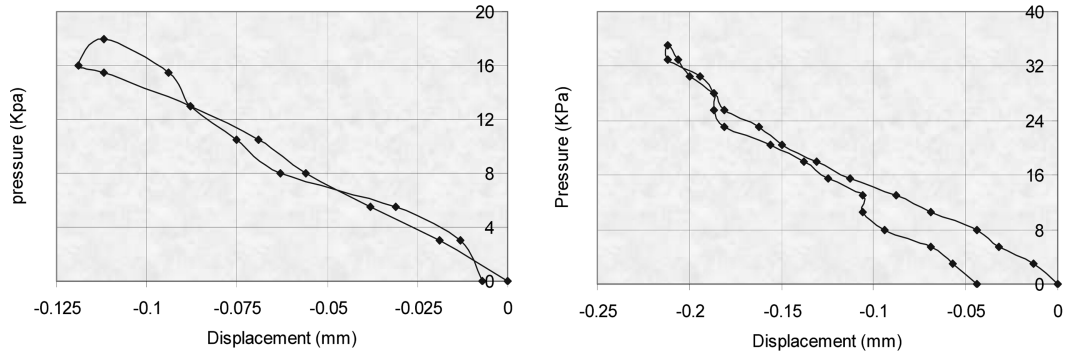

Fig. 5 Loading and unloading of specimens C and D

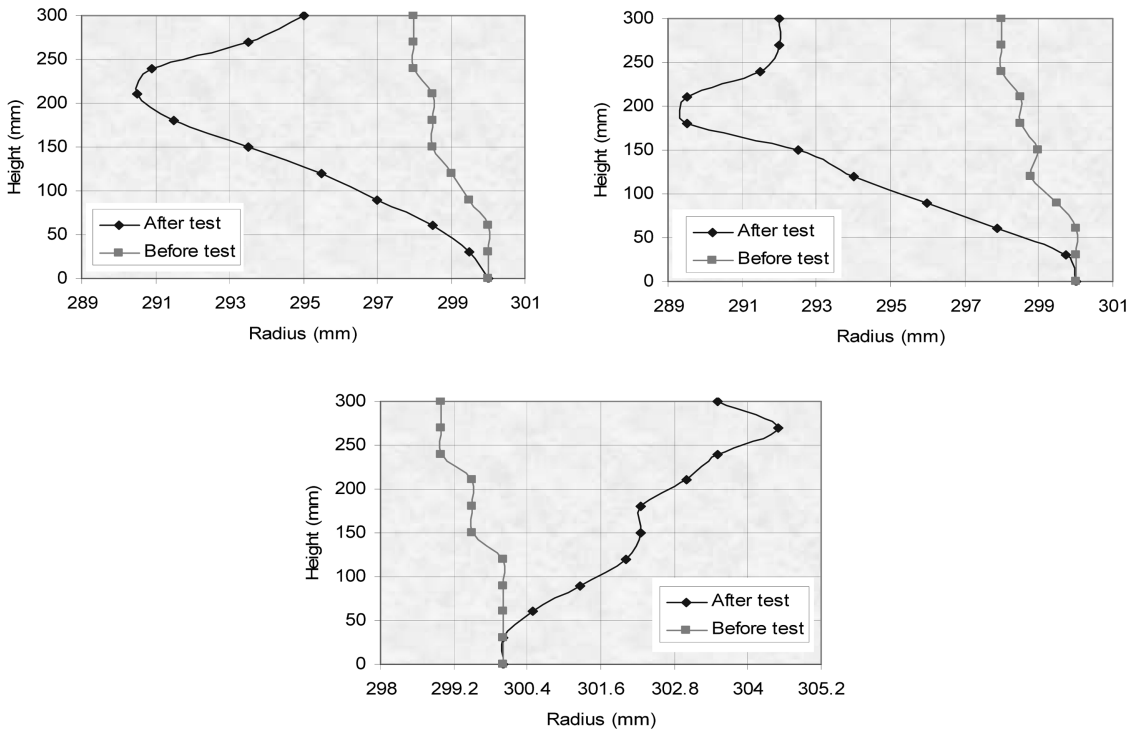

Fig. 6 Radial displacement of specimen A

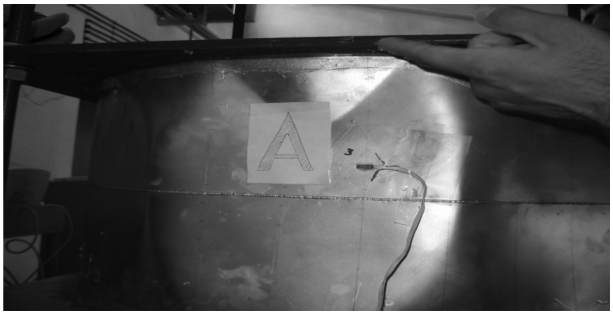

Fig. 7 “V” shape yield line in postbuckling range

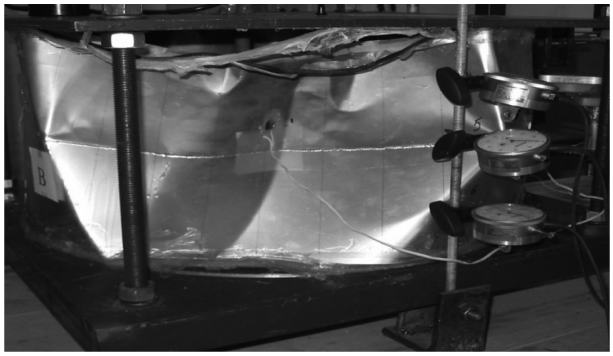

Fig. 8 Failure pattern of specimen B

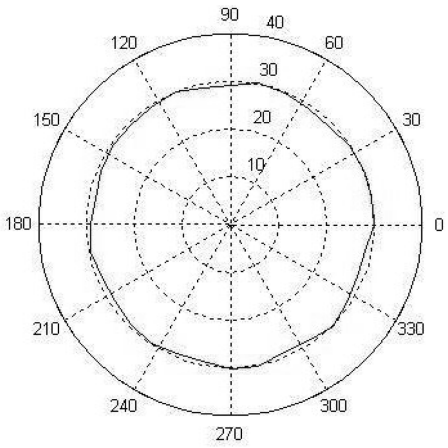

Fig. 9 Polar plot of final geometry measured on specimen D

Difference between initial buckling and overall buckling loads was considerable for all specimens. This point confirms the fact that a satisfactory post-buckling strength exists in this type of shells. It is observed a “V” shaped yield line was established in the region close to restrained edge of shells, before failure took place. The same phenomenon was observed in a separated experimental work reported by Showkati (1995). In Fig. 7 a typical behavior is pictured for specimen A.

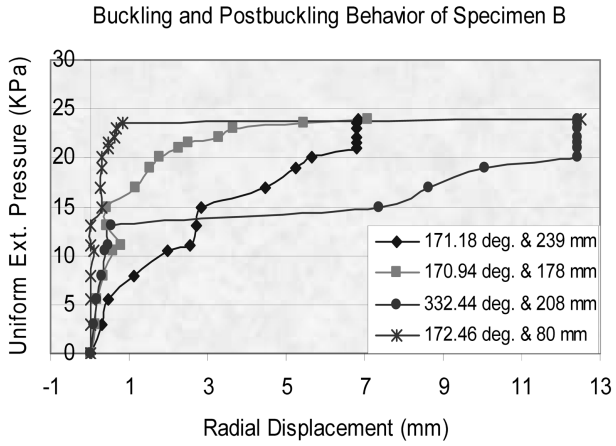

Fig. 10 Load-deformation graph for specimen B in different coordinates

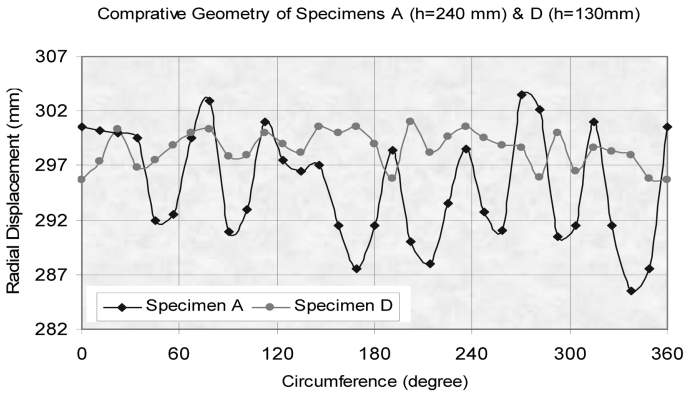

Fig. 11 Comparison the after test geometry of specimens A and D

By increasing the external pressure, the failure mode was gradually approached. In most specimens, occurrence a very large displacement in one edge caused an uncontrollable leakage on vacuum function and then the test stopped. Fig. 8 shows the failure of shell B clearly.

In the case of external pressure of cylindrical shells, the inward deformations are too larger than outward ones. It is a general characteristic of cylindrical shell buckling deformations to tend to go inwards. A comparable geometry of this fact in specimen D has been plotted in Fig. 9.

A graph of load-deformation path of test shell B is presented in Fig. 10 for buckling and postbuckling stages. It is evident from the results that thickness of the models has also dominant effect on the buckling and post-buckling behavior. The final deformation in thinner part of cylinder in all specimens is more than that of the thicker part. This phenomenon is more considerable in shells with high variation of thickness.

Final deformations of specimens A and B are higher than that of D and C, respectively because of higher *L/R* ratio of A and B (Fig. 11). Also, the higher *L/R* ratio decreases buckling capacity as well as the number of buckling waves. The difference between initial and overall buckling pressure was too much in all specimens. It means the cylindrical circular shells have a large post-buckling

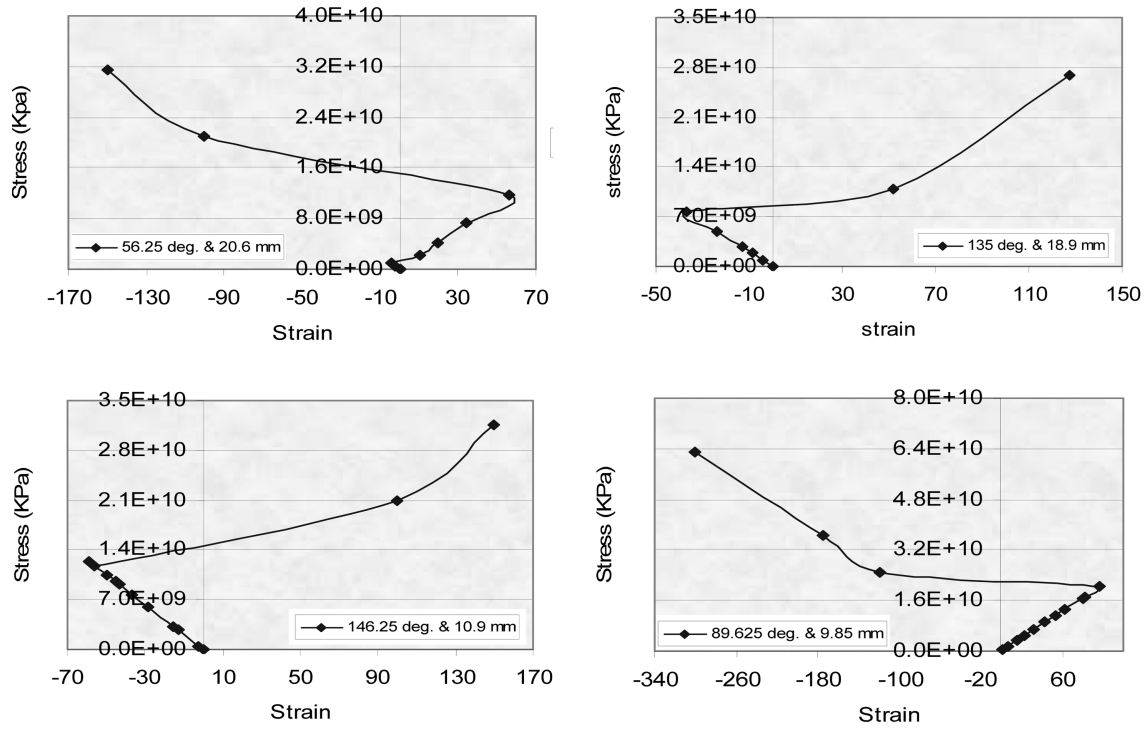

Fig. 12 Stress-strain graph for specimen A, B, C and D in different coordinates

capacity under external pressure. This fact has been clearly shown in Fig. 10 as well as in Table 3. In Fig. 12 Stress-strain graph for specimen A, B, C and D in different coordinates are shown.

4. Conclusions

The buckling and postbuckling behavior of cylindrical shells with varying thickness is experimentally investigated in this paper. The measured data and obtained results are reported for four specimens with simply supported ends under the effect of uniform external pressure. Each specimen has only one change in thickness along its length. The main concluding points are as follows.

- The initial buckling occurred simultaneously when one or more buckling lobes were established. Then the overall buckling mode has been formed by increasing the applied pressure.
- The yield lines at both ends of shell are in the form of "V" shaped in all specimens, which were established in the range of postbuckling.
- The inward deformations are so larger than the outward deformations due to external pressure.
- Existence of post-buckling strength was obviously evident in all specimens under the effect of uniform lateral pressure.
- The difference between initial and overall buckling loads was considerable indicating an extended region for post-buckling capacity.
- In the models with high thickness change, the final buckling waves were completely formed in

thinner part of the cylinders; however in the specimens with low thickness change, the waves were established in both parts of cylinders.

- It is experimentally confirmed the slender shells with higher ratio of *L/R* are more flexible in radial direction.
- The circumferential weld line has no effect on the geometry of meridian mode specially, when the thickness change is low.
- The longitudinal weld line causes the circumferential lobes to be unsymmetrical around the shell waist. Also it is evident that axial weld line is generally located at the beginning of a circumferential lobe.
- The theoretical buckling pressure and mode number are higher than the test results due to impossibility of full modeling of a physical shell by means of numerical tools. This discrepancy could be increased if the thickness change is present in the shell model

References

Aghajari, S. (2005), "Investigation of the buckling and postbuckling behavior of cylindrical shells with varying thickness under uniform external pressure", M. Eng Thesis, Faculty of Civil Engineering, Sahand University of Technology, Tabriz, Iran.

Ansourian, P. (1992), "On the buckling analysis and design of silos and tanks", *J. Constr. Steel Res.*, **23**, 273-294.

Batdorf, B. (1947), "A simplified method of elastic stability analysis for thin cylindrical shell, modified equilibrium equation", NACA TN 1342.

Donnell, L.H. (1933), *Stability of Thin-walled Tubes under Torsion, NACA Report*, No. 479.

Gadalla, M. and El Kadi, H. (2009), "Evaluation of thermal stability of quasi-isotropic composite/polymeric cylindrical structures under extreme climatic conditions", *J. Struct. Eng.,* **32**(3), 429-445.

Gusic, G., Combescure, A. and Jullien, J.F. (2000), "The influence of circumferential thickness variations on the buckling of cylindrical shells under external pressure", *Comput. Struct.*, **74**, 461-477.

Hansen, J.S. (1975), "Influence of general imperfections in axially loaded cylindrical shells", *Solid Struct.*, **11**, 1233-1243.

Hui, D. (1988), "Postbuckling behavior of infinite beams on elastic foundation using Koiter's improved theory", *Int. J. Nonlin. Mech.*, **23**(2), 113-123.

Holst, F.G., Rotter, J.M. and Calladine, C.R. (1999), "Imperfection in cylindrical shells resulting from fabrication misfits", *J. Eng. Mech.*, **125**(4), 410-418.

Koiter, W.T. (1967), "On the stability of elastic equilibrium", Doctoral Thesis, Delft, Amesterdam, 1945 (English Translation, NASA TT-10, 833).

Koiter, W.T. (1976), "General theory of mode interaction in stiffened plate and shell structures", Delft University of Technology, Report WTHD-91.

Koiter, W.T., Elishakov, I., Li, Y.W. and Starness, J.H. (1994), "Buckling of axially compressed cylindrical shell of variable thickness", *Int. J. Solids Struct.*, **31**(30), 797-805.

Lee, L.H. (1962), "Inelastic buckling of initially imperfect cylindrical shells subject to axial compression", *J. Aerosp. Sci.*, 87-95.

Li, Y.W., Elishakov, I., Starnes, J. and Bushnell, D. (1997), "Effect of thickness variation and initial imperfection on buckling of composite cylindrical shells: Asymptotic Analysis and Numerical Result by Bosor4 and Panda2", *Int. J. Solid Struct.*, **34**(28), 3755-3767.

Malik, Z., Morton, J. and Ruiz, C. (1980), "Buckling under normal pressure of cylindrical shells with various edge conditions", *J. Press. Ves. Tech.*, **102**, 107-111.

Popov, A.A. (2003), "Parametric resonance in cylindrical shells: a case study in nonlinear vibration of structural shell", *Eng. Struct.*, **25**, 789-799.

Portela, G. and Godoy, L.A. (2007), "Wind pressure and buckling of grouped steel tanks", *Wind Struct.,* **10**(1), 23-44.
Shen, H.S. and Chen, T.Y. (1991), "Buckling and post buckling behavior of cylindrical shells under combined external pressure and axial compression", *Thin Wall Struct.,* **12**, 321-334.
Showkati, H. (1995), "The buckling strength of cylindrical shells under external pressure", Ph.D. Thesis, The University of Sydney.
Winterstetter, T.A. and Schmidt, H. (2002), "Stability of circular cylindrical steel shells under combined loading", *Thin Wall. Struct.*, **40**, 893-909.
Yamaki, N. (1984), *Elastic Stability of Circular Cylindrical Shells*, Amsterdam, North-Holand.